

Stable algorithm for event detection in event-driven particle dynamics: Logical states

Severin Strobl · Marcus N. Bannerman · Thorsten Pöschel

Received: date / Accepted: date

Abstract Following the recent development of a stable event-detection algorithm for hard-sphere systems, the implications of more complex interaction models are examined. The relative location of particles leads to ambiguity when it is used to determine the interaction state of a particle in stepped potentials, such as the square-well model. To correctly predict the next event in these systems, the concept of an additional state that is tracked separately from the particle position is introduced and integrated into the stable algorithm for event detection.

Keywords DEM; Event-driven; Molecular dynamics; Square well; Stepped potential; Collision detection;

1 Introduction

Particle dynamics is the numerical solution for the motion of a collection of discrete bodies, each of which may represent objects ranging in size from atoms/molecules (molecular dynamics) to grains of sand or the ice in an avalanche (granular dynamics). There is a variety of particle dynamics approaches but common to all is the integration of Newton's equation of motion to determine the trajectory of the particles. Event-driven particle dynamics (EDPD) is one approach which integrates Newton's equation of motion exactly through piece-wise analytic solutions of the particle trajectories.

Severin Strobl · Thorsten Pöschel
Institute for Multiscale Simulation, Friedrich-Alexander-Universität Erlangen-Nürnberg, Nögelsbachstr. 49b, 91052 Erlangen, Germany
E-mail: severin.strobl@fau.de

Marcus N. Bannerman
School of Engineering, University of Aberdeen, Fraser Noble Building, AB24 3UE, United Kingdom

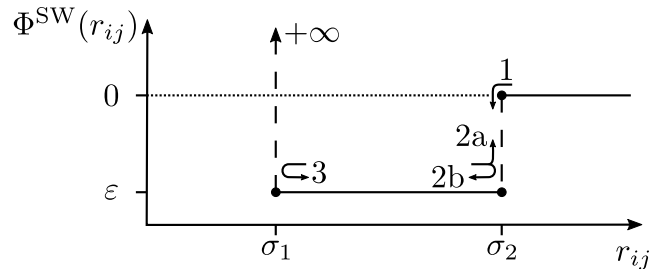


Fig. 1 The potential energy $\phi^{\text{SW}}(r_{ij})$ of the square-well model as a function of the separation distance, $r_{ij} = |\mathbf{r}_i - \mathbf{r}_j| \equiv |\mathbf{r}_i - \mathbf{r}_j|$, between two particles i and j . The inter-particle energy only changes in discrete steps at distances of $r_{ij} = \sigma_1$ and $r_{ij} = \sigma_2$. The numbered arrows indicate the four event types of the model generated by these steps: (1) Capture (enter the well), (2a) Release (escape the well), (2b) Bounce (remain in the well), and (3) Core (hard-sphere collision).

This avoids truncation error which arises if a numerical integration technique is used, but restricts the simulation to interactions where piece-wise analytic solutions can be found. One such class of compatible interactions are discrete potentials, such as the square-well model shown in Fig. 1. As there are no forces acting between discontinuities in the potential, the analytical solution to the dynamics is a simple ballistic motion of the particles. When particles cross a discontinuity, the instantaneous energy change results in an impulse and this *event* must be detected and processed at the exact time it occurs. The time of the next event is calculated *a priori* and the system is advanced forward in time directly to the instant of the event: i.e., the progression of time is event-driven. This allows EDPD implementations to be computationally efficient, particularly for dilute or stiff systems, as the uninteresting time between interactions and hence events is skipped.

In a recent paper [4] we demonstrated that the EDPD algorithm must be carefully constructed to ensure its numerical stability. Although the EDPD algorithm is exact, its implementation is sensitive to round-off error. In hard-sphere systems, round-off error manifests as overlapping/interpenetrating particles which is difficult to resolve as the dynamics is undefined in this state. If particles begin to interpenetrate, the stable algorithm executes additional events to ensure the interpenetrating particles do not continue to approach and, thus, increase their overlap [4]. Key to the stable algorithm is the definition of valid and invalid states but this distinction is only straightforward for hard interactions. For example, particles interacting via a square-well potential (see Fig. 1) may overlap ($r_{ij} < \sigma_1$) which is always an invalid state, but they can also be either in a *captured* state within ($\sigma_1 \leq r_{ij} \leq \sigma_2$) or an *uncaptured* state outside of the well ($r_{ij} \geq \sigma_2$). As a particle pair cannot energetically occupy both states, only one region is valid at a particular point in their trajectory. Thus, for stepped or multi-state interactions such as the square-well or stepped Lennard-Jones potentials [10], the valid state dynamically changes with time.

In this paper, the stable algorithm of Ref. [4] is extended to interactions with dynamically changing valid states. In Sec. 2, the numerically calculated position is demonstrated to be an unreliable indicator for the current state of the particle and additional logical state tracking is recommended. The extended stable algorithm for square wells is then outlined in Sec. 3. In Sec. 4, it is demonstrated that states must be tracked even for virtual/zero-impulse events. Finally, the tracking of states is validated for two example configurations in Sec. 5, illustrating the challenges with conventional approaches, before the conclusions are drawn in Sec. 6.

2 Ambiguity of particle state

When simulating systems with multiple valid states, it is crucial that the current valid state can be determined during the simulation in a reliable manner. The simplest approach is to try to use the position of the particles to compute the current state. Unfortunately, calculating the valid state this way is not always unambiguous. The difficulty stems from the fact that the captured state, $r_{ij} \in [\sigma_1, \sigma_2]$, and uncaptured state, $r_{ij} \in [\sigma_2, \infty)$, are both closed sets which include the point $r_{ij} = \sigma_2$. This is required as $r_{ij} = \sigma_2$ is the point of transition between the two states. As events are instantaneous, there can be no change in position during the transition. The ambiguity of particle state is thus not a numerical artifact, but is always encountered even in a precise simulation devoid of the peculiarities of floating point calculations.

To illustrate this further, consider the basic algorithm for the simulation of particles interacting via a square-well potential [1]:

1. For each particle pair:
 - (a) If they are uncaptured:
 - Test for capture events (type 1, compare Fig. 1).
 - (b) If they are captured:
 - Test for bounce/release (type 2) and core (type 3) events.
2. Sort the events to determine which one occurs first.
3. Move the system forward to the time of the first event, $t + \Delta t$.
4. For the interacting particle pair:
 - (a) If they are uncaptured:
 - Execute a capture event (type 1).
 - (b) If they are captured:
 - Execute a bounce/release (type 2) or core (type 3) event.
5. Return to step 1

In steps 1 and 4, the capture state of the particles must be determined. Consider the case where the next event to occur arises from the $r_{ij} = \sigma_2$ discontinuity and is either a capture or a release/bounce event. The particles will be moved in step 3 to the moment of interaction and will lie exactly on the well edge at $r_{ij} = \sigma_2$. At this point, the position has become ambiguous for testing the particle state and this failure occurs for all such events. In Fig. 2 two examples of square-well particles interacting via different event types are sketched. Independent of the original state (uncaptured or captured), during the event both particles have a separation distance $r_{ij} = \sigma_2$ leading to the ambiguity in the type of the event to execute.

In fact, in real implementations the ambiguity is not limited to a single point in the separation distance, but expands to an interval around the discontinuity due to the limited precision of floating point calculations. This is illustrated for hard spheres in Fig. 3 of Ref. [4] where particles moved during a core event have a distribution of separation distances, either slightly smaller or larger than the expected value. In square-well systems, this implies that particles moved into position for a well event will end up distributed both inside and outside of the well, regardless of which side they are on originally. While it might seem tempting to resolve the ambiguity at the discontinuity by taking into account the sign of the relative velocity in addition to the position of the particles, the distribution of the separation distance on both sides of the discontinuity impedes this approach.

The first published EDPD implementation by Alder and Wainwright [1] reduces the effects of this inaccuracy by storing the separation distance, r_{ij} , calculated

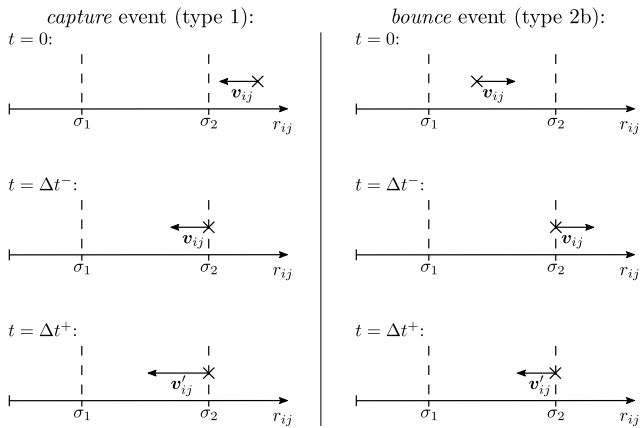


Fig. 2 Two configurations of a pair of particles i and j interacting via a square-well potential which lead to an ambiguity in the interaction state. The relative velocity $\mathbf{v}_{ij} \equiv \mathbf{v}_i - \mathbf{v}_j$ and its post-event value \mathbf{v}'_{ij} are indicated by the arrows. In the left case, uncaptured particles enter the well of the potential (event type 1 in Fig. 1) and their capture state changes. In the right case, two captured particles bounce on the well discontinuity (event type 2b in Fig. 1) and do not change their capture state. In both cases, the position before ($t = \Delta t^-$) and after ($t = \Delta t^+$) the event is identical, thus it cannot be used to determine the capture state immediately before or after an event.

in step 1 and uses it in step 4 to determine the capture state. As this separation is calculated before the particles are moved into place for the event there is a lower probability of failure; however, there is no inherent guarantee in this approach that the stored position calculated in step 1 is always unambiguous and free from error. The dynamics do not exclude particles from being located at or near a discontinuity during event detection. In fact, a particle which has just executed an event *must* be located near a discontinuity and ambiguity must arise immediately in the next iteration of step 1. Alder and Wainwright do not specify how event detection is carried out in this case [1].

There are a number of approaches in the literature which try to resolve the ambiguity arising from particles near to a discontinuity. One approach is to perform “corrections” to ensure that particles numerically transfer to the correct side of the discontinuity. This may be achieved through the addition or subtraction of a small quantity to the time of the next event [7]. Alternatively, the position may be directly changed to “nudge” the particles over the corresponding discontinuity after processing the current event (e.g., see the source code of Ref. [9]). Unfortunately, both methods rely on empirically determined correction factors, which depend on the system studied and may introduce other errors if another event occurs at around the same time. For example, if a third particle is in close proximity then

stretching the event time may cause an interaction to be missed.

The infinitely-thin hard rods system [5] is particularly interesting as it naturally exhibits a large number of repeated re-collisions between pairs of particles which have just collided. To prevent spurious re-detection of collisions which have just been executed, a minimum re-collision time computed from the underlying dynamics is enforced. This requires the storage of the last event of each particle to correctly apply the minimum re-collision time restriction. This approach is highly appealing as it uses some additional *logical* (not floating point) state to enforce that the correct system dynamics is generated.

It appears that, for systems where the valid states change with time, the simplest robust approach is to explicitly track the current state of particle pairs as additional logical information within the system. In square-well systems, the required logical state is boolean (“captured” or “uncaptured”) but in multi-step potentials there may be many logical states.

Initialization of the logical state may take place from the positional information only when the configuration is first generated (using an arbitrary choice to resolve the $r_{ij} = \sigma_2$ case). For all later times, the logical state must be stored and loaded along with the rest of the configurational information whenever the simulation is suspended or resumed. As the logical state only changes when the correct “transfer” event is executed, and only logically consistent events are tested, all ambiguity is eliminated. The stable implementation for square-well molecules is now outlined.

3 Stable event detection in square wells

The introduction of logical states requires some modifications to the stable algorithm for event detection as outlined in Ref. [4]. At the core of the stable algorithm lies the definition of an overlap function, $f(t)$, which indicates whether a pair of particles is in a valid state or not at the time t . The square-well system is composed of multiple applications of the overlap function f_{BB} for two closed balls, which has the following form:

$$f_{\text{BB}}(t + \Delta t, \sigma) = [\mathbf{r}_{ij}(t) + \Delta t \mathbf{v}_{ij}(t)]^2 - \sigma^2, \quad (1)$$

where $\mathbf{v}_{ij}(t) \equiv \mathbf{v}_i(t) - \mathbf{v}_j(t)$ is the relative velocity, and σ is the average diameter of the two balls. This function is negative if the balls are overlapping, positive if they are apart, and zero if they are in contact. Thus event detection for the intersection of two closed balls is transformed into the solution for the roots of f_{BB} .

The time derivative of an overlap function $\dot{f}(t)$ can be used to distinguish whether a currently invalid state

($f(t) < 0$) is either improving or stable in time ($\dot{f}(t) \geq 0$) or deteriorating ($\dot{f}(t) < 0$). For f_{BB} this corresponds to

$$\dot{f}_{\text{BB}}(t + \Delta t) = \mathbf{v}_{ij}(t) \cdot [\mathbf{r}_{ij}(t) + \Delta t \mathbf{v}_{ij}(t)]. \quad (2)$$

Following the algorithm in Ref. [4], a stable EDPD algorithm is defined as:

When testing for interactions between a pair of particles at a time, t , consider all logically valid overlap functions. For each overlap function, f , an event occurs after the smallest non-negative time interval, Δt , that satisfies the following condition:

$$\left(f(t + \Delta t) \leq 0 \right) \text{ and } \left(\dot{f}(t + \Delta t) < 0 \right). \quad (3)$$

This algorithm prevents errors in positional state from deteriorating once they are detected. If the two particles are uncaptured then only capture events are logically valid and are tested for using $f_{\text{BB}}(t, \sigma_2)$. If the two particles are already captured, then core events are tested for using $f_{\text{BB}}(t, \sigma_1)$ and release/bounce events must also be tested for using $-f_{\text{BB}}(t, \sigma_2)$. The negative of an overlap function is its inverse which results in $-f_{\text{BB}}$ becoming a test for when the particles will exceed the well distance σ_2 and become disjoint. Both core and bounce/release events are tested for at the same time and the earliest event is taken as the next event. As these functions represent distinct invalid state volumes in \mathbf{r}_{ij} , there is no chance of ambiguity through simultaneous events from both overlap functions. A reference implementation of the event-detection algorithm using the logical state and the corresponding overlap functions is given in Appendix A.

4 Virtual states

In Sec. 2, logical states are introduced for systems with dynamic valid states and applied in the context of discrete potentials. In these systems, the different logical states have a direct relationship to potential energy changes in the interaction potential; however, there are many cases where additional state tracking is desirable even though it is not associated with any physical action or impulse. These states may hence be considered as *virtual* states as they have no physical meaning. One example are neighbor-lists where the simulation domain is divided into small subvolumes or neighborhoods to optimise the search for the next event [8, 6]. Each neighborhood corresponds to a different virtual state for each particle, and only particle pairs in neighboring states are actually tested for events. It is vital that, even in these virtual state systems, the logical state is tracked and used to guarantee the correct dynamics.

The simplest example of this is a particle simulation where a virtual wall divides the simulation domain into two half-spaces. Virtual walls may be used to track transport properties such as the mass flux of particles across the wall, as well as form part of a neighbor-list implementation. The wall is virtual as it is merely a bookkeeping device and is penetrable by all particles. The wall divides the simulation space into two closed half-spaces. A suitable overlap function for one of these half-spaces is

$$f_{\text{HS}}(t + \Delta t) = \hat{\mathbf{n}} \cdot [\mathbf{r}_i(t + \Delta t) - \mathbf{c}], \quad (4)$$

where the half-space is defined by a normal $\hat{\mathbf{n}}$ perpendicular to the virtual wall and a point \mathbf{c} in the plane. The direction of the normal depends on which side of the wall the particle is currently on. As the overlap function is required to be positive for valid states, the normal must point into the half-space the particle is currently located in. If a particle is located either exactly or numerically close to the virtual wall it is unreliable to determine the current half-space (and hence the direction of the normal) from the position. Therefore the side of the wall the particle is located on must be tracked as additional logical state.

5 Validation

To illustrate the significance of state tracking, simulations of two model systems are performed. The first model is a square-well potential (Fig. 1) with parameters $\sigma_2 = 3\sigma_1$, and $\varepsilon = -k_B T$. The second model is an equivalent square-shoulder potential where $\varepsilon = +k_B T$. These potentials are the prototypes of more complex interaction models such as general stepped potentials [10]. Both simulations use $N = 32000$ particles and a reduced number density of $N\sigma_1^3/V = 10^{-3}$. Simulations are run for 10000 events per particle and an instrumented version of the DynamO [3] simulation package is used to collect statistics on inconsistencies which arise in the logical and physical state.

For the square-well system, the probability of inconsistencies arising during event processing is approximately 1.4×10^{-7} for each event, while for the square-shoulder system it is approximately 2.6×10^{-7} . Although these events occur relatively infrequently the results can be catastrophic. The implementation of Alder and Wainwright [1] becomes stuck and repeatedly executes identical release events (type 2a in Fig. 1). The simulation cannot proceed forward in time and the kinetic energy increases with each event. The logical states algorithm proposed here is able to continue the simulation and maintains the total energy to machine precision.

The rare nature of the inconsistency explains why it was not reported earlier in the literature; however, simulations of 10^{10} events or more (e.g., see Ref. [2]) are now commonplace, thus care must be taken to ensure the simulation remains unconditionally stable.

6 Conclusions

In conclusion, the physical and virtual state of an EDPD simulation must not be derived from the position of the particles except during initialisation. This information must instead be tracked as additional logical state and used to enforce that the correct event sequences are both detected and executed. The logical states represent a crucial part of the state of the system as a whole so, if the simulation is suspended, all logical states must be stored and restored accordingly once the simulation is restarted. During the runtime of the EDPD simulation the logical states must only evolve via the execution of the correct transfer events. For example, for the previously examined square-well model, only the event types 1 and 2a (Fig. 1) for particles entering or leaving the square well lead to a change in the logical state for this pairing of particles.

Unlike the configurational state (which is inherent to each particle in the system), logical state may be required for each possible pairing of interacting particles. Thus the number of stored states may scale as $\mathcal{O}(N^2)$ in the number of particles, N . To avoid difficulties in scaling to large systems, efficient hashed implementations are recommended where only variations from the most common state are stored. Typically, this reduces the required storage to $\mathcal{O}(N)$.

If the idea of logical states is combined with the stable algorithm for event detection, inherently stable EDPD simulations are possible. This is shown in Sec. 5 for simulations of systems using square-well or square-shoulder potentials. Furthermore simulations of more complex interaction models without any artificial modification of the list of predicted events or interference with the dynamics of the system are enabled.

Acknowledgements The authors gratefully acknowledge the support of the German Research Foundation (DFG) through the Cluster of Excellence 'Engineering of Advanced Materials' at the University of Erlangen-Nuremberg and through grant Po 472/25.

A Stable algorithm for square-well molecules

The calculation of the event times in Sec. 3 is expressed in terms of the ball-ball overlap function, f_{BB} , as given in Eq. 1. This operation is especially sensitive to round-off error in the

floating point representation, therefore two numerically robust subroutines which analyse f_{BB} are presented here. Both use the quadratic equation to solve for the roots of f_{BB} ; however, each has different safeguards against numerical errors. The first algorithm, **BallBallIntersectionTime** (Algorithm 1), calculates the time until two balls begin to intersect. The second, **BallBallDisjointTime** (Algorithm 2), calculates the time until two balls become disjoint. Both subroutines return $+\infty$ if no event is detected and use the appropriate numerically stable form of the quadratic equation.

Function BallBallIntersectionTime($\mathbf{r}_{ij}, \mathbf{v}_{ij}, \sigma$)

```

 $a \leftarrow \mathbf{v}_{ij} \cdot \mathbf{v}_{ij}$ 
 $b \leftarrow \mathbf{r}_{ij} \cdot \mathbf{v}_{ij}$ 
 $c \leftarrow \mathbf{r}_{ij} \cdot \mathbf{r}_{ij} - \sigma^2$ 
 $arg \leftarrow b^2 - ac$ 
if  $b \geq 0$  or  $arg \leq 0$  then return  $+\infty$  return  $\max(0,$ 
 $c / (\sqrt{arg} - b))$ 

```

Algorithm 1: A stable algorithm for detection when two initially disjoint balls begin to intersect. In terms of the overlap function, this determines the time until $f_{BB} \leq 0$ and $\dot{f}_{BB} < 0$ or returns $+\infty$ if this does not occur in the future.

Function BallBallDisjointTime($\mathbf{r}_{ij}, \mathbf{v}_{ij}, \sigma$)

```

 $a \leftarrow \mathbf{v}_{ij} \cdot \mathbf{v}_{ij}$ 
 $b \leftarrow \mathbf{r}_{ij} \cdot \mathbf{v}_{ij}$ 
 $c \leftarrow \mathbf{r}_{ij} \cdot \mathbf{r}_{ij} - \sigma^2$ 
 $arg \leftarrow b^2 - ac$ 
if  $a = 0$  then return  $+\infty$  if  $arg \leq 0$  then return
 $\max(0, -b/a)$  if  $b > 0$  then
| return  $\max(0, (\sqrt{arg} - b) / a)$ 
else
| return  $\max(0, -c / (\sqrt{arg} + b))$ 
end

```

Algorithm 2: A stable algorithm for detecting when two initially intersecting balls become disjoint. This determines the time until $f_{BB} \geq 0$ and $\dot{f}_{BB} > 0$ or returns $+\infty$ if this does not occur in the future.

The introduction of the logical state and the overlap function requires some changes to the detection of events as outlined in step 1 of the basic algorithm given in Sec. 2. The modified algorithm is presented in **SWEEventTime** (Algorithm 3). The logical state is required as input to this function and must be tracked separately. For the square-well model, this is a single Boolean value per particle pair indicating whether the particles are captured or not. The specialized routines of Algorithms 1 and 2 are then used to determine the roots of the overlap function. In the case of a captured particle pair, both discontinuities at σ_1 and σ_2 are accessible and the minimum of the respective event times has to be selected.

References

1. Alder, B.J., Wainwright, T.E.: Studies in molecular dynamics. 1. General method. J. Chem. Phys. **31**(2), 459–466 (1959). DOI 10.1063/1.1730376

```

Function SWEventTime( $\mathbf{r}_{ij}$ ,  $\mathbf{v}_{ij}$ ,  $\sigma_1$ ,  $\sigma_2$ , captured)
if captured then
   $\Delta t_1 \leftarrow$  BallBallIntersectionTime( $\mathbf{r}_{ij}$ ,  $\mathbf{v}_{ij}$ ,  $\sigma_1$ )
   $\Delta t_2 \leftarrow$  BallBallDisjointTime( $\mathbf{r}_{ij}$ ,  $\mathbf{v}_{ij}$ ,  $\sigma_2$ )
  return min( $\Delta t_1$ ,  $\Delta t_2$ )
else
  return BallBallIntersectionTime( $\mathbf{r}_{ij}$ ,  $\mathbf{v}_{ij}$ ,  $\sigma_2$ )
end

```

Algorithm 3: The stable EDPD algorithm for event detection between two square-well particles i and j .

2. Bannerman, M.N., Lue, L., Woodcock, L.V.: Thermodynamic pressures for hard spheres and closed-virial equation-of-state. *J. Chem. Phys.* **132**, 084,507 (2010). DOI 10.1063/1.3328823
3. Bannerman, M.N., Sargant, R., Lue, L.: Dynamo: A free O(N) general event-driven simulator. *J. Comp. Chem.* **32**, 3329–3338 (2011). DOI 10.1002/jcc.21915
4. Bannerman, M.N., Strobl, S., Formella, A., Pöschel, T.: Stable algorithm for event detection in event-driven particle dynamics. *Comp. Part. Mech.* **1**, 1–2 (2014). DOI 10.1007/s40571-014-0021-8
5. Frenkel, D., Maguire, J.F.: Molecular dynamics study of the dynamical properties of an assembly of infinitely thin hard rods. *Mol. Phys.* **49**(3), 503–541 (1983). DOI 10.1080/00268978300101331
6. Marín, M., Risso, D., Cordero, P.: Efficient algorithms for many-body hard particle molecular-dynamics. *J. Comput. Phys.* **109**(2), 306–317 (1993). DOI 10.1006/jcph.1993.1219
7. Pöschel, T., Schwager, T.: *Computational Granular Dynamics*. Springer-Verlag, Berlin Heidelberg (2005). DOI 10.1007/3-540-27720-X
8. Rapaport, D.C.: Event scheduling problem in molecular dynamics simulation. *J. Comput. Phys.* **34**(2), 184–201 (1980). DOI 10.1016/0021-9991(80)90104-7
9. Schultz, A.J., Kofke, D.A.: Etomica: An object-oriented framework for molecular simulation. *Journal of Computational Chemistry* **36**(8), 573–583 (2015). DOI 10.1002/jcc.23823
10. Thomson, C., Lue, L., Bannerman, M.N.: Mapping continuous potentials to discrete forms. *J. Chem. Phys.* **140**, 034,105 (2014). DOI 10.1063/1.4861669